Active Vibration Damping in the Presence of Uncertainties

Travis Eisenhour[1], Sam Hatchett[2], and Isaac Salazar[3]

[1] Department of Aerospace & Mechanical Engineering, Notre Dame University, Notre Dame, IN, 46556
[2] Department of Mechanical Engineering, Texas Tech. University, Lubbock, TX, 79409
[3] Department of Mechanical Engineering, Texas A&M, College Station, TX, 77843

ABSTRACT

Several control design techniques including PID, LQG, and PPF are investigated for active vibration damping of a cantilever beam with uncertain boundary conditions. Step disturbances were used to evaluate the performance of the designed controllers.

NOMENCLATURE

C	Controller or compensator
E	Elastic Modulus (Pa)
f_j	Natural frequency (Hz)
GA	Genetic Algorithm
I	Area Moment of Inertia (m^4)
LQG	Linear Quadratic Gaussian
M	End mass (added to beam) (kg)
P	Plant (physical system)
PID	Proportional Integral Derivative
PPF	Positive Position Feedback
PZT	Piezoelectric Transducer
QFT	Quantitative Feedback Theory
ω_j	Natural frequency of the system (rad/s)
ζ	Damping ratio of the system

Superscript

T	Transpose of Matrix

Analytical Solution Nomenclature

m	Mass per unit length (kg/m)
ℓ	Length of beam (m)
w	Lateral displacement of beam (m)
x	Distance (axial) down beam (m)
β	Solution parameter

LQG Nomenclature

A	Matrix in system's state space equation
B	Column vector in system's state space equation
C	Row vector in measurement equation
J	Performance Index
K	Optimal Gain Matrix
L	Observer Gain Matrix
Q	Parameter in cost function
R	Parameter in cost function
u	Control states (input to system)
v	Measured noise
w	Input noise
x	State vector (states of the system)
x_e	Estimated state vector
y	Measured states

PID Nomenclature

b	Damping constant
e	Error measurement
F	Resultant controller output
k	Stiffness
K_d	Derivative gain
K_i	Integral gain
K_p	Proportional gain
m	Mass

PPF Nomenclature

b	Level of force into the mode of interest
c	Simplification of "g / b"
g	Controller constant
q	Controller degree of freedom
u	Input to system (out of controller)
U(s)	Laplace transform of u
x	System degree of freedom
X(s)	Laplace transform of x
ω_{nf}	Natural frequency of the controller (rad/s)
ζ_{nf}	Damping ratio of the controller

1. INTRODUCTION

Many structures may change in the course of their operation, yet still be required to fulfill their design purpose. A specific example relates to the vibrations experienced by the wings on a B52 aircraft. Without active control, the amplitudes of vibration would be unacceptably high while flying at low altitudes. However, since fuel is stored in the wings, the vibration characteristics of the aircraft change during the course of flight; thus any control architecture must be capable of compensating for uncertain system parameters. Another example concerns interceptor missiles, which use maneuvering thrusters to track a target. The thrusters cause

vibrations in the missile body, which affect the tracking accuracy of the seeker head. In addition, the missile body's vibration characteristics change as fuel is consumed.

The objective of this study is to design, implement, and compare active vibration control architectures for a cantilevered aluminum beam. These controllers are also compared under the presence of uncertainties by adding end mass. Proportional Integral Derivative (PID), Linear Quadratic Gaussian (LQG), and Positive Position Feedback (PPF) are the architectures explored in this study.

A number of references for general control system design theory exist, such as [1] and [2]. Also, there are more detailed studies on particular controller architectures. PID has a variety of applications and has been used with numerous systems. Kashani discusses applying LQG to a flexible plate [3]. For a comparison of PPF (active control) and parallel resistor-inductor shunt technique, [4] is a good source.

2. CONTROLS AND CONTROL MODEL DESIGN

In a simple feedback system, as shown in Figure 2.1, the plant is the system to be controlled.

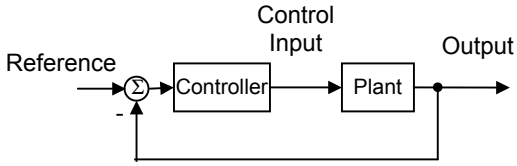

Figure 2.1 – Schematic of a simple feedback system.

The controller or compensator, C(s), is designed to force the plant P(s) to have a desired response. The transfer function for the system without any feedback is called the open loop transfer function. In the above diagram the open loop transfer function is defined as $P(s)C(s)$. The closed loop transfer function from reference input to output is:

$$\frac{P(s)C(s)}{1+P(s)C(s)} \qquad (2.1)$$

In a feedback control system, the output is measured by a sensor and fed into the controller to influence the controller response. There are numerous control architectures available in the design of an effective controller. The three architectures being compared in this study are the following: Proportional Integral Derivative (PID), Linear Quadratic Gaussian (LQG), and Positive Position Feedback (PPF).

2.1. PID CONTROL DESIGN

PID (proportional, integral, derivative) controllers are quite popular for their robustness and ease of implementation. A PID controller tracks the system error; its integral; and its derivative, applies gains to each of these terms, sums these new terms, and outputs the result to the plant.

2.2. LQG CONTROL DESIGN

One advantage of state-space optimal control design is that it consists of a series of independent steps. First, the definition of a control law allows the resulting closed-loop system to attain satisfactory transient response. If the full state of the system is not available, an estimator (sometimes called an observer), which computes an estimate of the entire state vector when provided with the system's measurements [1], is used. The final step is to combine the control law and the estimator. Figure 2.2 shows how the control law and the estimator are combined to form a compensator. Linear Quadratic Gaussian (LQG) is one type of state-space optimal control design.

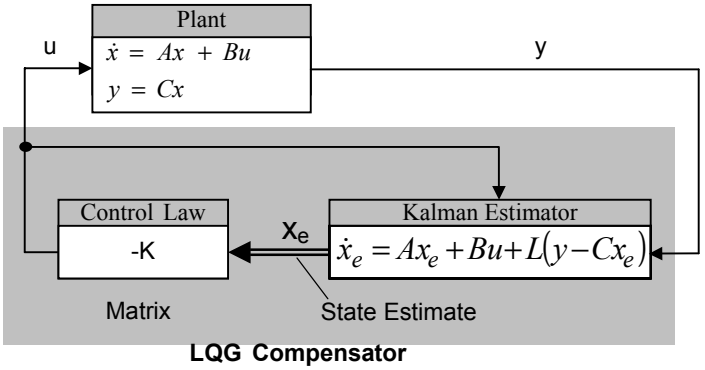

Figure 2.2 – Schematic of LQG state-space design.

2.3. PPF CONTROL DESIGN

Some controller architectures do not require a system model in their design. Positive Position Feedback (PPF) controllers are an example of this controller type. An advantage of PPF controllers is that only the resonant frequencies and the system's low-frequency gain are required to design the compensator [5]. Advantageously, this controller architecture is not sensitive to spillover, where contributions from unmodeled modes affect the control of the modes of interest. However, designing a controller for each mode may be difficult [6]. A major aspect of concern for all controllers is stability. Friswell and Inman [6] cover stability of PPF in detail when applied to single and multiple degree of freedom models. An important characteristic to note is that stability is not dependent on the controller damping ratio. Another difference between PPF and most other controllers is that the feedback of the output to the controller is positive, whereas this feedback is negative in other controllers. Figure 2.3 shows the PPF block diagram.

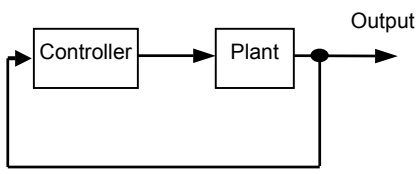

Figure 2.3 – Schematic of PPF feedback system.

3. PIEZOELECTRICS

Piezoelectric materials generate an electric charge proportional to applied stress, which makes them a natural sensor. Conversely, piezoelectric materials can be effectively used as an actuator, as they deform when an electrical charge is applied. The piezoelectric actuators obtained from PCB Piezotronics Inc. (item 713A01) have a frequency range of 0 to 50 kHz. At the 100-v maximum voltage the patch can produce approximately 21 N of actuation force. The patch actuator used in this study measured 4.3 x 0.84 x 0.05 inches (109 x 21.3 x 1.27 mm). When applied in a closed-loop control system, the patch actuators develop a canceling force to reduce vibration.

4. EXPERIMENTAL DESCRIPTION

The system under consideration is a cantilevered 6061 Aluminum beam of dimensions 24 x 2 x 0.25 in (61 mm x 6 mm x 51 mm) with a variable mass at the free end.

4.1. EXPERIMENTAL CONFIGURATION

Two piezoelectric patches mounted on opposite sides of the beam 140 mm away from the fixed end are used as a sensor and actuator. The signal from the sensing piezoelectric patch is fed through a voltage divider so the signal conditioning hardware is not saturated with the high voltage output.

The data acquisition setup consists of a National Instruments PCI-6052E signal conditioner connected to a real time operating system. Software needed to run the data acquisition included MATLAB, Simulink, Real-Time Workshop, and a C compiler. When a test is run, a Simulink model is compiled and connected to the real time OS via the network using Matlab xPC Target software.

See Figure 4.1 for a picture of the experimental setup. Following are the labeled parts:

(a) National Instruments PCI-6052E signal conditioner

(b) Voltage divider

(c) Piezoelectric Patches (one on each side)

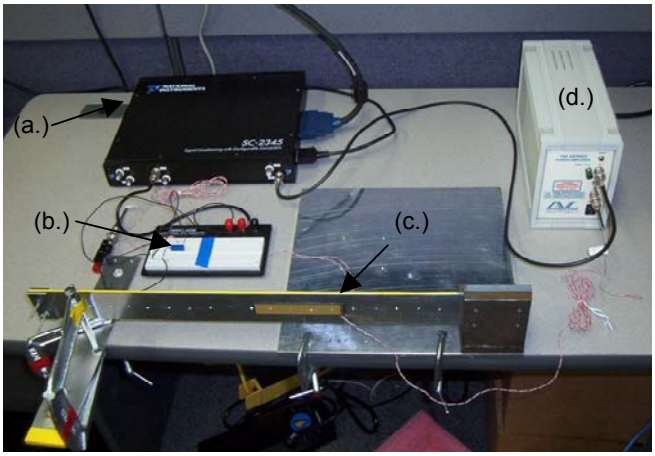

Figure 4.1 – Picture of experimental setup

(d) AVC Instrumentation 790 Series Power Amplifier

4.2. EXPERIMENTAL PROCEDURE

System identification tests, finite element results, and closed form solutions are compared for three end-mass cases (0.00, 64.3, 129 grams). Using modal data obtained from the system identification tests, an estimate of the input to output transfer function is produced. The control design consists of comparing results from three different design techniques in their ability to reduce vibration in the nominal case (no end-mass). Finally, a stability check in the presence of uncertainty (variable end mass) is used to determine robustness characteristics of each controller.

5. ANALYSIS OF BEAM

To aid in control design, the system's natural frequencies need to be found. Analytical solution and the finite element method can be used to estimate the natural frequencies. The natural frequencies can also be measured experimentally.

5.1. ANALYTICAL SOLUTION

For the analytical solution (or exact solution), the beam is modeled as a continuous system. See Figure 5.1 for a sketch of the analytical model.

The equation of motion and boundary condition for a beam

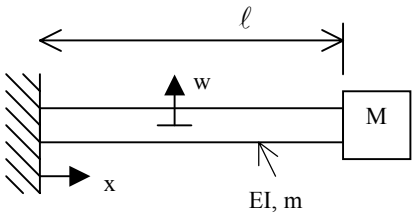

Figure 5.1 – Sketch of analytical model of the beam.

in transverse vibration with end mass can be found in most vibration textbooks, i.e. [7]. The boundary conditions are applied to the general solution of the equation of motion assuming separation of variables, leading to the characteristic equation:

$$\mathrm{EI}\beta^3\left(1+\cosh\beta\ell\cos\beta\ell\right) + \omega^2\mathrm{M}\left(\sinh\beta\ell\cos\beta\ell+\cosh\beta\ell\sin\beta\ell\right) = 0 \qquad (5.1.a)$$

$$\text{, where } \beta^4 = \frac{m}{\mathrm{EI}}\omega^2 \qquad (5.1.b)$$

Solving the characteristic equation for ω gives the natural frequencies of the model of the beam. Appropriate values can be substituted for M to vary the end mass. The results from the analytical solution are tabulated in Section 5.4.

5.2. FINITE ELEMENT SOLUTION

To evaluate the mode shapes and frequencies with finite element tools, Abaqus CAE is used. Within Abaqus, a model with the same measurements as the actual beam is constructed. Material properties are selected in accord with the physical system (Aluminum 6061), and a clamped

boundary condition is imposed on the rear face. Using a 10-node Modified Quadratic Tetrahedron mesh (standard element library) and 3-D stress analysis, the model is evaluated for the first three bending modes of the cantilever. The first three mode shapes are shown in Figure 5.1.

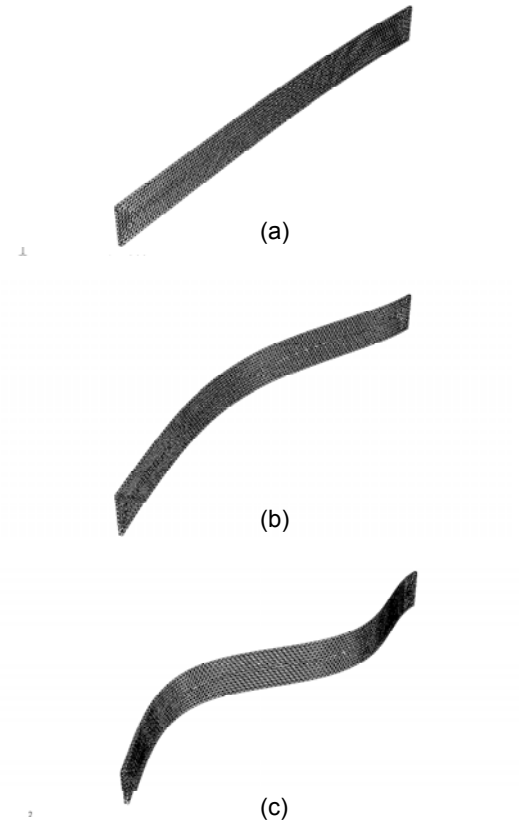

Figure 5.1 – Mode shapes from FE model: (a) first mode, (b) second mode, and (c) third mode.

5.3. EXPERIMENTAL RESULTS

To determine the true natural frequencies of the beam, the process and system described in Section 4 are used. Random excitation is input by one of the piezoelectric patches (PZT). The other PZT is used as a sensor. The frequency response function (FRF) is found from the input and output data (time domain). See Figure 5.2. The natural frequencies of the beam can be extracted from the FRF.

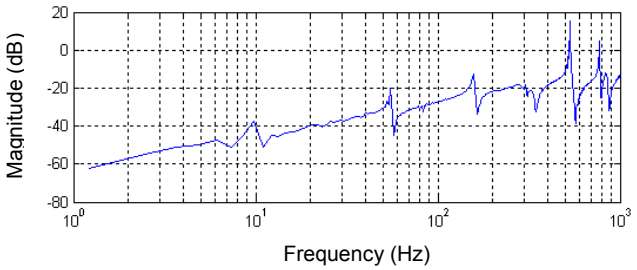

Figure 5.2 – Plot of experimental FRF

5.4. COMPARISON OF NATURAL FREQUENCIES

The natural frequencies of the beam are determined using the aforementioned methods. These methods are applied for three different cases: nominal (no end mass), 65-gram end mass, and 130-gram end mass. Table 1 lists the results of the beam analysis.

Table 5.1 – The natural frequencies (Hz) for the three cases.

	f_1	f_2	f_3
Nominal			
Analytical	9.11	57.1	160
Abaqus	10.0	62.8	176
Actual	9.31	55.0	157
65-gram end mass			
Analytical	4.87	43.2	133
Abaqus	7.20	52.8	157
Actual	6.56	44.9	138
130-gram end mass			
Analytical	3.71	41.8	132
Abaqus	5.91	50.2	132
Actual	5.34	42.6	134

6. APPLICATION OF PID CONTROL

The mathematical realization of a PID controller is

$$F = K_P e + K_D \dot{e} + K_I \int_0^t e dt \,, \qquad (6.1)$$

where e is the error measurement, F is the resultant output, and K_p, K_i, and K_D are the proportional, integral, and derivative gains, respectively. Differentiating (6.1) once with respect to time,

$$\dot{F} = K_P \dot{e} + K_D \ddot{e} + K_I e \,, \qquad (6.1)$$

and taking the Laplace transform,

$$sF = (K_D s^2 + K_P s + K_D) e \,, \qquad (6.2)$$

the resulting transfer function *(F/e)* for a PID controller is

$$C(s) = \frac{K_D s^2 + K_P s + K_I}{s} \,. \qquad (6.3)$$

To pick the optimal gain terms for the controller based on frequency and damping criteria, the denominator of the closed-loop transfer function of the system is set equal to the desired expression in the Laplace domain. The denominator of the closed-loop transfer function is

$$s^3 + \frac{b + K_D}{m} s^2 + \frac{k + K_P}{m} s + \frac{K_I}{m} \,, \qquad (6.4)$$

where *m*, *b*, and *k* are the mass, damping, and stiffness terms, respectively. This expression is then set to be equal to

$$(s+10\zeta\omega_n)(s^2+2\zeta\omega_n+\omega_n^2), \qquad (6.5)$$

where ζ and ω are the damping and frequencies derived from the desired criteria (i.e. settling time, time to rise, etc.). The extra root at $-10\zeta\omega$ is added to satisfy the third-order transfer function denominator. Adding this extra root has very little effect on the desired results, as it lies far above the frequencies of interest. With the equation

$$s^3+\frac{b+K_D}{m}s^2+\frac{k+K_P}{m}s+\frac{K_I}{m} = (s+10\zeta\omega_n)(s^2+2\zeta\omega_n+\omega_n^2) \qquad (6.6)$$

the PID gains can be determined.

For the system under consideration, a slightly different technique is used to determine acceptable PID gain values. A Genetic Algorithm (GA) is employed to perturb multiple solutions and find the fittest combination of gains.

Genetic Algorithm is a term used to describe a set of steps used to either maximize or minimize a specific function, which is referred to a 'fitness function' [8]. A typical GA begins with an initial population of solutions. The population is comprised of a specifiable number of members, which can be scalars or vectors. The GA evaluates the fitness function at each member of the initial population and records the results. It then separates the fittest of these members and discards the others. The fittest members are used to repopulate the set and are randomly perturbed within specified boundary limits. The fitnesses of these new members are evaluated and the procedure is repeated for a specified number of cycles [8].

In the case of the cantilever beam, the fitness function is comprised of three inputs (the PID gains) and one output (settling time). Built into the function is a sixth order transfer function approximation based on experimental data. Each time the fitness function is called, it generates a PID transfer function based on its inputs and evaluates the impulse response of the closed-loop system. The function outputs the settling time as the fitness to be minimized.

7. APPLICATION OF LQG CONTROL

For this study, a Kalman estimator provides the optimal state estimate of the system. When the Kalman estimator is used, the method is known as Linear Quadratic Gaussian (LQG). The LQG method is a linear optimal full state feedback control technique that minimizes the impulse response and control expenditure in a quadratic sense [3]. Given the system of equations:

$$\dot{x} = Ax + Bu + w \quad \text{(system)} \qquad (7.1.a)$$

$$y = Cx + v \quad \text{(measurement),} \qquad (7.1.b)$$

where A, B, and C are a matrix, column vector and row vector in a system's state space representation. Variables w and v are the process and measurement noise respectively. The steps involved in the design of an LQG controller are the following. First calculate the optimal gain matrix K so the state feedback law $u = -Kx$ minimizes the cost function: [1]

$$J = \int_0^\infty x^T Q x + u^T R u \, dt, \qquad (7.2)$$

where Q and R are cost function parameters, x is the output, and u is the input. Second, use the Kalman filter equation [2] to estimate the state x_e and calculate the observer gain matrix L. The result is an optimal state estimate that is fed back to the system. Finally, apply the state-feedback and observer gains K & L to the system by making the following substitutions in equations 7.1.a and 7.1.b:

$$A = [A-BK-LC] \qquad (7.3.a)$$

$$B = L \qquad (7.3.b)$$

$$C = -K, \qquad (7.3.c)$$

while setting w and v = 0.

8. APPLICATION OF PPF CONTROL

In order to study PPF controllers, the equations used to represent the compensator is given by:

$$\ddot{q} + 2\zeta_f \omega_{nf} \dot{q} + \omega_{nf}^2 q = \sqrt{g}\,\omega_{nf}^2 x \qquad (8.1.a)$$

$$u = \frac{\sqrt{g}}{b}\omega_{nf}^2 q \qquad (8.1.b)$$

The simplest way to implement this in Simulink is to use the controller's transfer function (u/x). Taking the Laplace Transform of (8.1) results in the following equation:

$$TF = \frac{U(s)}{X(s)} = \frac{c\,\omega_{nf}^4}{s^2 + 2\zeta_f \omega_{nf} + \omega_{nf}^2} \qquad (8.2.a)$$

$$\text{, where } c = \frac{g}{b} \qquad (8.2.b)$$

By applying a PPF controller to a multiple degree of freedom system with just one controller input, a beneficial facet becomes obvious. The high frequency response should not be fed into a PPF controller. The controller has a much greater effect when this is done.

Another use of the transfer function is to check stability using the Bode plot, as described in Section 2. To do this, the experimental frequency response function (FRF) needs to be found, and the transfer function needs to be converted to the frequency domain (substitute $s = j\omega$). Then, at each

frequency the experimental FRF and the model of the controller in the frequency domain are multiplied together; this is the open loop FRF. Now this can be done in order to check the stability for various controller parameters (ω_{nf}, ζ_f, c). While the parameters that result in stable systems may not function properly when implemented, they give a starting point.

9. COMPARISON OF RESULTS

For the PID, LQG, and PPF controllers designed, the settling times are compared using a 2% criterion. The time it takes for the response to settle within 2% of the maximum amplitude defines 2% criterion. This comparison is first done for the nominal system and then for the end mass cases.

9.1. OUTCOME FOR NOMINAL SYSTEM

In the nominal case, the uncontrolled settling time was 26 seconds. The PID controller proved to be effective, causing a 67% reduction in settling time. Unfortunately, the LQG controller did not perform as desired and reduced settling time by only 21%. (See Section 9.3.) On the other hand, the PPF controller proved to be very effective, reducing settling time by 87%. Figure 9.1 shows a comparison of the performance of each controller with the same step condition applied.

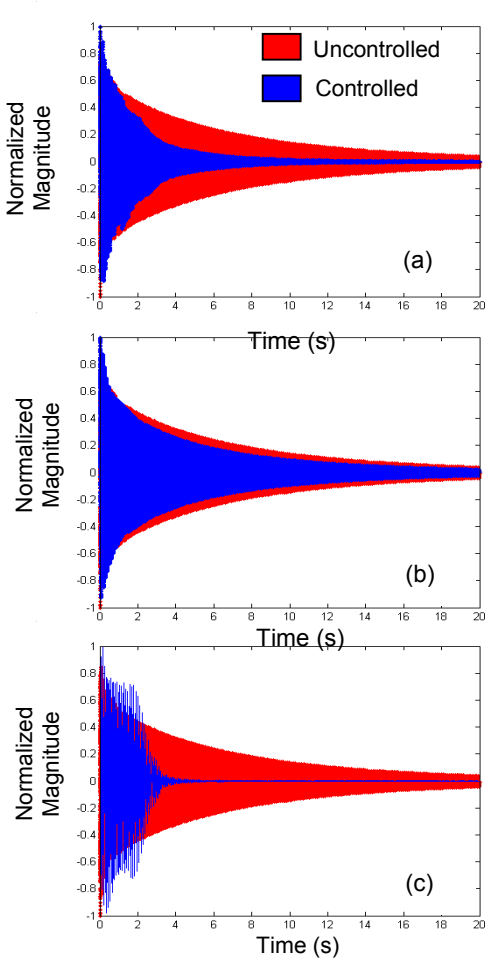

Figure 9.1 – Nominal response comparison for (a) PID, (b) LQG, and (c) PPF controllers.

9.2. DISCUSSION OF ROBUSTNESS

When checking the controllers' robustness characteristics, the control design for the nominal case is used. Intentionally introduced uncertainty in the form of end masses had noticeable effects. The PID controller proved to be marginally stable and unstable for the 65-gram and 130-gram end mass cases, respectively. In the 65-gram case, the PID controlled system sustains a small amplitude of vibration, referred to as a limit cycle, and did not settle to 2% of the maximum amplitude within the window of interest (the first 30 seconds). Similarly, the 130-gram end mass controlled system entered a limit cycle, and in fact the controller caused the beam to repeatedly impact the C-clamp. Figure 9.2 shows the comparison of the uncontrolled and controlled response for the PID controller.

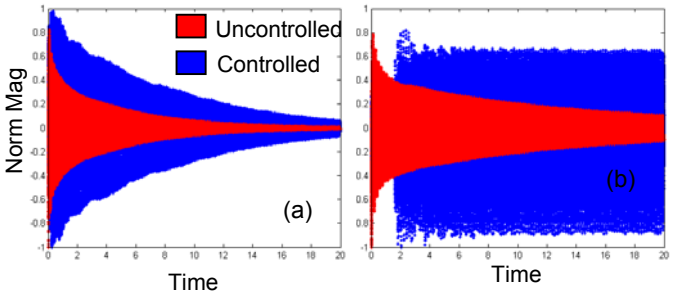

Figure 9.2 – PID controller comparison for the (a) 65-gram case and (b) 130 gram case.

The LQG controlled beam showed slightly greater settling times for the 65-gram and 130-gram end mass cases. That the system did not show signs of instability with the end masses attached was encouraging. See Figure 9.3 for LQG

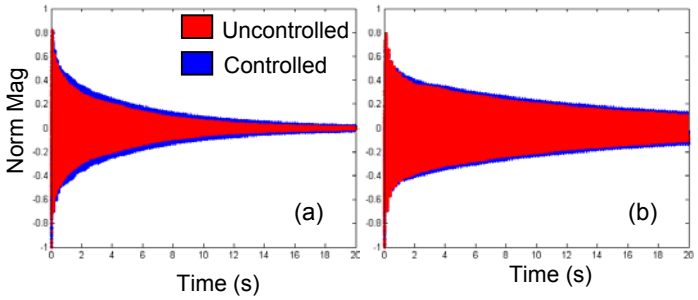

Figure 9.3 – LQG controller comparison for the (a) 65-gram case and (b) 130 gram case.

response comparisons.

Surprisingly, the PPF controller did not perform well in the presence of uncertainty. In the 65-gram case, the system entered a limit cycle after transients died out near 14 seconds. Likewise, in the 130-gram end mass case, the system entered a limit cycle and sustained high magnitude of vibration. Figure 9.4 shows response comparisons for the PPF controller.

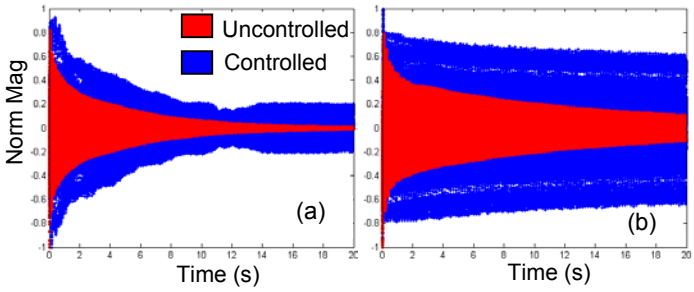

Figure 9.4 – PPF controller comparison for the (a) 65-gram case and (b) 130 gram case

9.3. LQG IMPLEMENTATION ISSUES

A state-space control design with a state observer must be observable and controllable. Observability refers to the ability of the controller to estimate a state variable. A system described by the matrices (**A,B**) can be said to be controllable if there exists an unconstrained control u that can transfer any initial state x(0) to any other desired location x(t) [9]. One can determine controllability by checking if the rank of the matrix [B AB A^2B …$A^{n-1}B$] is equal to the number of states in the system. A transfer function that described the input to output FRF closely through the first seven natural frequencies (11^{th} order) is used in the design of an LQG controller. The state-space representation of the 11^{th} order approximation is found to be neither controllable nor observable. Because of this problem, a reduced approximation of the transfer function is used to create a state space representation. Because the LQG design requires an accurate transfer function, the resulting LQG controller performed significantly different than anticipated.

10. SUMMARY

This study shows that vibration control design for a nominal case may not always be sufficient for all structures. If damage occurs, boundary conditions change, material properties change, or another perturbation in the system occurs, the controller may not work properly, and in some cases may cause the system to become unstable. As fuel stored in the wings of a B-52 is used, the vibration characteristics will change. Robustness characteristics must be checked to determine if the control design is sufficient in the presence of uncertainty. In addition, if a control system is to be designed for multiple, nominally similar systems, variability in the population should be considered in the control design.

Recommendations for further research:

1. Apply robust design methods, such as Quantitative Feedback Theory (QFT), to address uncertainty.
2. Compare effectiveness of piezo patches that apply moment and piezo patches that apply an axial force.
3. Conduct similar experiments on different systems.
4. Evaluate the effects of saturation.

11. ACKNOWLEDGMENTS

This research project was preformed at Los Alamos National Laboratory as part of the Third Annual Los Alamos Dynamics Summer School (LADSS). The funding for this work was provided by the Engineering Science and Applications Division and by The Department of Energy's Education Programs Office. The authors would also like to thank their mentor, Matt Bement, for his assistance and Charles Farrar for coordinating the summer school. The following companies generously provided various software packages that were necessary to complete the student projects: Vibrant Technologies (experimental modal analysis software); The Mathworks, Inc. (numerical analysis software); and Hibbitt, Karlsson and Sorensen, Inc. (ABAQUS finite element software).

12. REFERENCES

[1] Franklin, G.F., Powell, D.J., Emami-Naeini, A., Feedback Control of Dynamic Systems, Third Edition, Addison-Wesley Publishing Company, 1994.

[2] Belanger, Control Engineering: A Modern Approach, International Thomson Publishing, 1995.

[3] Kashani, R., Active Vibration Damping using Optimal Control Techniques, www.deicon.com/vib_tutorial/act_vib3_pdf.pdf

[4] DeGuilio, A.P., "A Comprehensive Experimental Evaluation of Actively Controlled Piezoceramics with Positive Position Feedback for Structural Damping," M.S. Thesis, Virginia Polytechnic Institute and State University, Blacksburg, Virginia, 2000.

[5] Farinholt, K, and Leo, D.J., Active Acoustic Attenuation for Launch Vehicles, Virginia Tech, Blacksburg, Virginia, 2002.

[6] Friswell, M, and Inman, D.J., "The relationship between positive position feedback and output feedback controllers," Smart Materials and Structures, v. 8, pp. 285-291, 1999.

[7] Rao, S.S., Mechanical Vibrations, Third Edition, Addison-Wesley Publishing Company, Reading, Massachusetts, 1995.

[8] Houck, C.R., James, J., and Kay, J., Binary and Real-valued Simulation Evaluation for Matlab, 1996.

[9] Dorf, R.C., Bishop, R.H., Modern Control Systems, Ninth Edition, Prentice-Hall, Inc., Upper Saddle River, New Jersey, 2001.